Technical Report

The Next Best Touch or Non-Touch: Object Pose Estimation via Sculpting with Compliant Hands

Alexander Rietzler[1], Carlos J. Rosales[2], Marco Gabiccini[2], Justus Piater[1]

***Abstract*— Many robotic tasks rely on the ability of a vision system to accurately estimate the 6 dimensional pose of objects in a scene. In many cases a single vision sensor does not provide sufficient information to discriminate a single correct pose of an object. This work solves the problem of refining the pose distribution of an object solely via proprioceptive sensing of occupancy. Our main novel contribution is an algorithm that plans a robot arm-hand trajectory such that information gathered about the object pose belief is maximized while at the same time impact on the object is minimized. This may result in actions that do not make contact with the object at all. Impact on the object is further reduced by using a compliant robotic hand. In this report our the theoretical foundations of our ongoing work are presented and intermediate results are shown.**

I. INTRODUCTION

Typically, robotic manipulation tasks like grasping rely on a pose estimate of an object in a scene. In the real world there is always uncertainty associated with the pose of an object. Reasons for that can be related to vision sensors like imperfect sensor calibration or low sensor resolution. Objects that are made of materials like glass can be undetectable for many 3-D vision sensors. Uncertainty in object pose can also arise from an incomplete view of the object, which creates occlusion and thus ambiguity in object pose that also humans cannot resolve without further action.

Consider a motivating scenario as depicted in Fig. 1. Due to self-occlusion we experience ambiguity in the position of the handle of a mug. By probing hypotheses at certain positions with a robotic hand we are able to exclude overlapping pose hypotheses.

This is an example where a robot equipped with position sensors is able to measure the metric space it occupies. Since this space must be free, the robot can infer that no other physical object occupies the same space. We can use this reasoning to plan a robotic trajectory for gaining information about the pose distribution of an object of interest. The main contribution of our work is a framework for planning for a robot action that maximizes expected proprioceptive information gain on object pose belief while simultaneously minimizing movement of the object as a results of the robotic hand touching it. As an adaptive hand we use the anthropomorphic Pisa-IIT Softhand [4]. An advantage of this hand is its simple control due to its single actuated degree of freedom. Particularly useful in our case is that it adapts its fingers mechanically to the object in while covering a large space with its fingers. This adaption mechanism ensures that compared to a robot hand with stiff fingers, the contact forces get mechanically distributed between the fingers which leads to low impact on the objects positioning. Also the hand is very robust and therefore ideal to operate it in a uncertain environment. In our scenario we make the assumption that we have a scene containing a single object. This object is of known shape, which implies that we have a pointcloud model available.

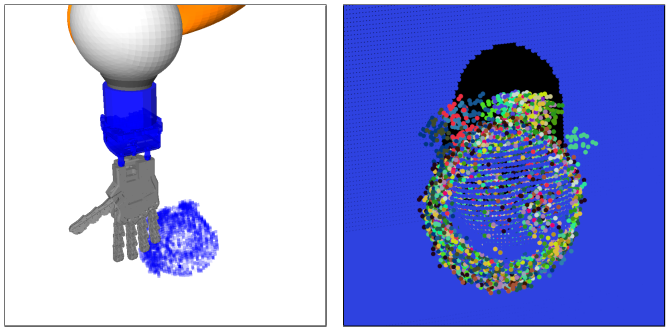

Fig. 1: Robot performing an information gathering action to refine the pose belief of a mug. The uncertainty in pose arises due to self-occlusion of the mug's handle.

The scene is captured with a Kinect sensor, which provides us with a pointcloud. We use a standard pose estimation algorithm [7] to sample a probability density over object pose. The density is represented nonparametrically by a particle set, which allows us to model the pose distribution to as much detail as necessary. This is particularly relevant in our scenario where we "poke dips" into our pose distribution by locally-applied information-gathering actions.

In order to compute an action we exploit both the pose distribution and an occupancy grid representation. The occupancy grid is built both by integrating sensor measurements and by updating it through object pose hypotheses. This

[1]Alexander Rietzler and Justus Piater are with the Institute of Computer Science, Technikerstrasse 21a, University of Innsbruck, Austria {alexander.rietzler,justus.piater}@uibk.ac.at

[2]Carlos J. Rosales and Marco Gabiccini are with the Centro di Ricerca "E. Piaggio", Univ. di Pisa, Italy. Email: carlos.rosales@for.unipi.it

The research leading to these results has received funding from the European Community's Seventh Framework Programme FP7/2007-2013 (Specific Programme Cooperation, Theme 3, Information and Communication Technologies) under grant agreement no. 600918, PaCMan.

representation allows us to compute the probability of the robot to make contact with an object faster than checking contact with each of the pose hypothesis individually. The link between occupancy grid and object pose distribution is established in a Bayesian fashion via a graphical model introduced by Wong et al. [16]. The model will be detailed in Sec. III-C.

Our information-gathering actions are parametrized by a cartesian trajectory for the robotic hand's wrist and open-close states for the actuated degrees of freedom. To infer an action we search in the space of reachable endeffector poses. In the next step we rank all the action starting at the endeffector positions by expected information gain. The information gain is computed using the Kullback-Leibler divergence between hypothesized posterior and prior pose belief. The expectation is build over the anticipated time an action lasts. An action stops due to reaching two different stopping thresholds, either by having a too large wrench offset measured with a wrist-mounted force-torque sensor or if the robotic hand joints offset measured with respect to its expected configurations is too large. We manually set these thresholds during forward simulation of the action such that we can minimize object movement at execution time.

After executing the action we update the pose distribution and re-plan actions until the entropy of the pose belief reaches a certain value.

II. RELATED WORK

The use of information gain to select a robot action has been extensively studied in the active vision community. In this field the authors present algorithms for computing robot-camera movements that improve object tracking [5], surface model generation [11], object recognition and pose estimation [2], [12].

In the case of selecting actions based on tactile information gain, robot-environment interaction has to be taken into account. Hebert et. al. [9] have introduced a method to select the next best touching action to localize the 3D object position or other object model parameters. Similar to our work they choose an action from a set of predefined candidate actions. To update the belief over object parameters they use a combined measurement model that is based on both binary contact detection and tactile sensors. In contrast, we use only proprioceptive measurements of occupancy, which enables us to gain information when we do not interact with the object at all. Instead of using information gain, Hsiao et. al. [10] use a decision-theoretic approach and an approximate POMDP to select actions for tactile exploration.

Other authors select an action for reducing object pose uncertainty while simultanously fulfilling a second constraint. Zito et. al. [17] plan a sequence of actions that distinguish hypothesized object states from competing ones while also reaching a goal configuration, in their case a force-closure grasping configuration. To compute a trajectory, they modify the cost function of a PRM planner by including a metric that measures the difference between contact observations expected at the most likely object pose and contact observations at all other hypotheses. By trading off information gain and execution time, a recent work of Tosi et. al. [15] provides the user with deterministic influence over on the length of every sensing action.

There are a few publications that use haptic measurements for pose estimation. Early works [8], [1] use solely tactile measurements or already integrate tactile with vision to recognize and localize polyhedral object models using simple matching algorithms. More recent works tackle more complex problems. Strub et. al. [14] estimate an objects pose during in-hand manipulation sequences. Others combine vision and more sensor modalities including force sensing, tactile and proprioception [3], or focus more on the computational tractability of computing a realtime update of a 6DOF pose posterior distribution modeled with particles [13]. Recent work from Wong et. al. [16] combines the occupancy grid representation and object-based representations like belief over an object's pose and identity in a general way. They illustrate a motivating example where they use contact-free proprioceptive measurements of an robot arm to update an occupancy grid and subsequently are able to distinguish between two different objects. We extend there work in the sense that we also gain information purely by proprioception, but in contrast we provide an automated way to compute a robot action to do so.

III. METHOD

Our paper is concerned with finding a robot *action* that helps localizing an object's pose. We focus on scenarios in which the uncertainty in the pose of the object naturally arises from occlusion. This can lead to anisotropic pose belief distributions as the occluded regions allow certain object parts to hide in occluded space. As a result we need to model the belief distribution as non-Gaussian.

If uncertainty in the object state is above a certain threshold, an action search is triggered. The action that maximizes information gain is executed and the belief distribution updated using aquired measurements. This process is repeated until the threshold reached.

In this Section we describe the full process starting from estimating the object's pose belief distribution to estimation of the information gain.

A. Pose Belief Distribution - Prior

To compute the distribution of a single object given scene observations we use an extension of the existing method by Detry et al. [7], [6], which represents a pose distribution as a kernel density estimate.

Let $A = \{a_i\}$ and $B = \{b_i\}$ with $a_i \in \mathbb{R}^3$ and $b_i \in \mathbb{R}^3$ be the pointcloud representation of object and scene.

A measure of overlap is used to define the belief of a pose hypothesis. This overlap is defined as the cross-correlation between continuous surface distributions that are generated from the pointclouds using kernel density estimation.

$$p(x) = N \int_{\mathbb{R}^3} \phi_A(t_x(y))\phi_B(y)dy, \tag{1}$$

where N is a normalizer and $\phi(y)$ are the kernel density estimates that are computed as a mixture of Gaussians. The rigid body transformation of object model points is denoted by $t_x(\cdot)$ where x is a pose $\in SE(3)$. This integral is estimated by Monte-Carlo approximation. We make use of the above equation to sample a pose distribution by using simulated annealing on a Markov chain. We reject samples with a probability below a certain threshold for computational reasons.

B. Pose Belief Distribution - Posterior with Respect to Occupancy

Our algorithm to sample the pose belief distribution does not prevent object hypotheses from penetrating free space. By integrating our measurements from a RGBD-sensor via ray-tracing into a 3-D occupancy grid, we are able to represent free space. All grid cells have their occupancy probability modeled independently. The state of the j^{th} cell is described with $m_j \in \{0, 1\}$ and with prior probability $p(m_j = 1) = \psi$. Following the Bayesian formulation by Wong et. al. [16], we compute the pose belief distribution posterior with respect to a set of occupancy measurements $\hat{z} = \{z_{1:Z}\}$ by re-weighting the pose samples. By Bayes' rule,

$$p(x|\hat{z}) \propto p(\hat{z}|x)p(x), \tag{2}$$

$$p(\hat{z}|x) \propto \frac{1}{\psi} \prod_{j \in J(x)} p(m_j = 1|\hat{z}_{(j)}). \tag{3}$$

Here $p(m_j = 1|\hat{z}_{(j)})$ are the grid cell occupancy probabilities with integrated measurements. The (j) in expression $\hat{z}_{(j)}$ denotes that only measurements relevant for the occupancy of cell j are considered. The product runs over all grid cells $J(x)$ which are overlapping by the object model surface transformed under pose hypothesis x. For small occupancy probabilities, the product converges to zero fast. This strongly reduces weight of hypotheses penetrating free space.

C. Occupancy Grid Posterior and Cell-to-Hypotheses Lookup Table

To compute a suitable robot action we do need to check collisions between the rigid links of the robot and the object. Instead of checking collision with hypothesized pointcloud models we project all of them into a single occupancy grid. Following Wong et. al. [16], we update the occupancy grid based on the pose belief. Intuitively we can imagine that if hypothesized object model points overlap a certain grid cell, this cell will then increase its occupancy likelihood proportional to the probability of the object hypothesis. Mathematically this connection can be written as

$$p(m_j|\hat{z}) = \sum_x p(m_j|x, \hat{z}_{(j)})p(x|\hat{z}), \tag{4}$$

$$p(m_j|x, \hat{z}_{(j)}) = \begin{cases} 1 & \text{if } j \in J(x) \\ p(m_j|\hat{z}_{(j)}) & \text{otherwise} \end{cases} \tag{5}$$

Our measurements to gain information about the pose belief distribution consists of proprioceptive contact measurements. As we have a large number of hypotheses this computation is expensive. To speed up the computation we associate each cell j of the occupancy grid with all colliding object model hypotheses. This results in a cell-to-hypotheses lookup-table that maps each grid cell's j to a set of hypotheses indexed by i, where $i \in I_{\text{all}}$. In addition we need to compute all the contact normals at the contact point in order to simulate the dynamic behavior of the adaptive robotic hand. A second lookup table is defined to find corresponding contact normals $n_{i,j}$ at the position of the cell . The lookup-tables are defined as

$$I: \ j \mapsto I(j), \tag{6}$$

$$n: \ (i, j) \mapsto n_{i,j}, \tag{7}$$

where $I(j)$ denotes the set that for a given cell id j contains the l_j hypotheses with $(0 < l_j < |I_{\text{all}}|)$. Note that $I(j)$ is in a sense the inverse of $J(x)$ from equation 3 because $J(x)$ are all grid cells overlapping by object in pose x and $I(j)$ are all object hypotheses overlapping with grid cell j. The computation time saved is a factor in the order of the average number of pose hypotheses associated with a grid cell.

D. Pose Belief distribution - Update under Action

Our implementation assumes deterministic dynamics of the robot and object state. Therefore, we can simply update the pose belief distribution in the same way as in equation 2, except that we change notation because we assume that measurements $\hat{z}$ are taken under action a_i at a certain timestep t. By Baye's rule,

$$p_{\text{t+1}}(x|\hat{z}, a_i) = \frac{p_t(\hat{z}|x, a_i)p_t(x)}{\int p_t(\hat{z}|x, a_i)p_t(x)\,\mathrm{d}x}. \tag{8}$$

The implemented measurement model $p_t(\hat{z}|x, a_i)$ is the same as in equation 3 except for the difference that we can only measure if a grid cell is not occupied as we cannot interpenetrate with any physical object in reality. Our measurements $\hat{z}$ are proprioceptive measurements of occupancy and are integrated into the occupancy grid cell via a the following measurement model

$$p(m_j = 0|\hat{z} = x^R) = 1 - \beta \text{ if the robot collides cell } j,$$
$$p(m_j = 1|\hat{z} = x^R) = \beta \text{ if the robot collides cell } j, \tag{9}$$

where x^R is the state of the robot and β is the false positive error rate.

E. Action - Parametrization

The actions are parametrized in form of a robot-state trajectory. The trajectory is divided into two segments. The first segment describes the free-space path of the current robot-state from its current state to the pre-action state. This trajectory segment is planned by a generic trajectory planner.

The second segment describes the interactive part, It starts in the pre-action state and aims to end in the vicinity or in contact with the object.

The second segment, which we from now on refer to as action, is parametrized in form of a cartesian path associated to the wrist of the robotic hand and by open and close state for the actuated degree of freedom of the hand.

Different actions consist of a set of manually defined movements that we call action primitives, examples are shown in Fig. 2.

In order to find a new action, 6 DOF cartesian endeffector poses for the pre-action state are sampled and checked against reachability and collision with the environment. Each action is then tested for executability of the cartesian path and ranked with respect to expected information gain.

F. Action - Stopping Criteria

Actions are executed on the real robot or in simulation. We assume that the object is movable and we also want to prevent our robot from damage when exploring the unknown environment. Therefore, we stop the robot if the 6-axis force-torque sensor connected to the wrist of the robotic hand reads a high wrench offset. Another second termination condition is reached if the joint position offset, the difference between measured and commanded joint position, reaches a manually defined threshold. We write the joint position and wrench offsets as

$$\Delta q = \|q_{\text{mes}} - q_0\|_{M_q}, \text{with } M_q = \text{diag}\left(\frac{1}{\sigma_{q_i}^2}\right) \tag{10}$$

$$\Delta\omega = \|f_{\text{mes}} - f_0\| + \frac{1}{\lambda}\|\tau_{\text{mes}} - \tau_0\|. \tag{11}$$

Here, the q_{mes} denotes the joint configuration of the adaptive hand under influence of contact, whereas q_0 would be the the contact-free configuration. To weight the different joints, the norm is taken under a Mahalanobis metric with a $n \times n$ diagonal Matrix M_q, where n is the number of joints. The diagonal entries of the matrix are comprised of the variances in measured joint configurations of the hand when operated on the real robot or on simulation. We trade-off between forces and torques when computing the norm of the wrench difference to account for difference in the dimension of these physical quantities. Therefore, we set λ to $0.2\,m$ as this is roughly the distance from the origin of the force torque sensor to the expected contact points on the robotic hand, leading to similar values of forces and torques.

G. Action - Probability of not Having Stopped

In order to compute expected information gain we also need to takethe probability of an action not having stopped before τ into account. Here τ parametrizes the progress in space or time of the robot action trajectory.

Compared to real execution we have to predict the dynamic behavior of our robot given that it interacts with the object in pose x. In our implementation we need the algorithm to be fast, so instead of using a physics simulator we approximate the dynamics. To simulate reaching of the force-torque offset threshold, we simply measure collision between all stiff and rigid links of the robot and the object model. We denote collision with a binary function $\Gamma(x, x^R) \in \{0, 1\}$, where x^R is the full state of the robot.

To simulate the joint configuration offset, we first need to predict the adaptive hand's joint configuration under influence of contact. In our case we use the Pisa-IIT hand, which is an underactuated hand built by the model of adaptive synergies [4]. The configuration of the hand is computed as

$$q_{\text{sim}} = A(E, R, J^T)f_c + B(E, R)\sigma^{(k)}, \tag{12}$$

where E are joint space stiffness matrices, R is the transmission ratios matrix and J^T the jacobian transpose, f_c are all contact forces and $\sigma^{(k)}$ the reduced synergy vector that describes the motor state of the actuated degrees of freedom. The matrix functions A and B are combining different linear combinations of the matrices. The computational intense part is to get the list of contact forces f_c. We approximate them by assuming unit force magnitude and by using the contact normals $n_{i,j}$ that appear at collision of object hypotheses and robot. They are computed from the lookup tables, see equations 6 and 7.

We model the likelihood of stopping the action given that object is in state x and that the robot is in state x_τ^R at time τ. We denote the state of stopping the action as $\overline{s}$.

$$p(\overline{s}|x, x_\tau^R) = \begin{cases} 1 & \text{if } \Gamma(x, x_\tau^R) = 1 \\ 1 & \text{if } \Delta q_{\text{sim}} > q_{\text{thres}} \\ 0 & \text{otherwise} \end{cases} \tag{13}$$

Marginalization over all object hypotheses gives us the likelihood of stopping the action at time τ.

$$p(\overline{s}|x_\tau^R) = \int p(\overline{s}|x, x_\tau^R)p(x)\,\mathrm{d}x \tag{14}$$

In the next step we want to compute the probability density of not *having* stopped the action *until* time $\hat{\tau}$ along the trajectory. As the probability of not having stopped implies that it could not have stopped at any point time before $\tau = \hat{\tau}$, we can factorize the expression above over all timesteps τ.

$$p(\overline{s}|\hat{\tau}) = N\frac{1}{\tau_{\max}}\prod_{\tau=0}^{\hat{\tau}} p(\overline{s}|x, x_\tau^R)^{\mathrm{d}\tau} \tag{15}$$

Here, N is a normalizer and $\frac{1}{\tau_{\max}} = p(\tau)$ is a uniform prior over timesteps . We can use this probability density to compute the expectation of the information gain under the condition that we did not stop the action.

H. Information Gain

As a measure of reduction of uncertainty in the pose belief distribution we use the information theoretical measure of relative entropy of the posterior with respect to prior, also Kullback-Leibler divergence of the posterior, or information gain. Given that the measurement takes time until $\hat{\tau}$, we can write the information gained until this time as

$$IG(\hat{\tau}) = \int p_{t+\hat{\tau}}(x)\log\left(\frac{p_{t+\hat{\tau}}(x)}{p_t(x)}\right)\mathrm{d}x, \tag{16}$$

$$IG(\hat{\tau}) = \int_{\tau=0}^{\hat{\tau}} \frac{\mathrm{d}}{\mathrm{d}\tau}\left(IG(\tau)\right)\mathrm{d}\tau. \tag{17}$$

In the second equation we write the differential information gain, which is the increment of information gain measured at time $\hat{\tau}$. Please note that in our implementation we directly compute a discrete version of the differential gain and thus do not need to perform any analytical differentiation. Our task is to find the next best action a^*, for which the measurements $\hat{z}$ made to update the prior belief distribution are hypothetical. This means that we forward simulate the measurements of each action and compute the information gain given this action. In addition we do not know when the action stops, so we also consider the probability of not having the stopped the action until a certain timestep $\hat{\tau}$ into account.

Building the expectation and inserting equation 2 gives.

$$E_{\hat{\tau}}[IG(\hat{\tau}, a_i)] = \tag{18}$$
$$\int p(\overline{s}|\hat{\tau}) \frac{\mathrm{d}}{\mathrm{d}\hat{\tau}} \left(\int p_{\mathrm{t}+\hat{\tau}}(x|\hat{z}, a_i) \log \left(\frac{p_{\mathrm{t}+\hat{\tau}}(x|\hat{z}, a_i)}{p_t(x)} \right) \mathrm{d}x \right) \mathrm{d}\hat{\tau}$$

The best action is then selected by taking the arg max of the expected information gain.

$$a^* = \arg\max_{a_i} E_{\hat{\tau}}[IG(\hat{\tau}, a_i)] \tag{19}$$

IV. CURRENT EXPERIMENTAL PROGRESS

In the following, we describe the progress made so far. As a first step, the pose distribution sampling has been successfully implemented.

Figure 1 shows 34 pose samples in different colors that have been sampled using equation 1 and re-weighted using equation 3. Due to computational simplifications and discretization issues we remove hypotheses having a weight below a certain threshold. We also rescaled the object model to about 95% of its normal size during collision checking with the occupancy grid, to remove many false positive collision detections that arise because many points potentially overlap with free grid cells that lie in the vicinity of the visible object surface, as one can see for the mug example.

In the next step, the computation of the occupancy grid posterior has also successfully been implemented using equation 4. Figure 2(d) shows a top-view of the occupancy grid posterior of the mug. As a prior a uniform occupancy has been assumed, so no visual observations have been integrated. In the implmentation the actual occupancy probability of a certain grid cell depends a lot on the sampling resolution of the object model. In our case we use 500 model points. As shown in the Figure, this might lead to many voxels having a low occupancy although they are close to voxels that would have already been measured as fully occupied visually.

Also we defined the action primitives. We defined three primitives to show the capabilities of using an adaptive hand in this task. One can see a visualization of them in Fig. 2. The spring action is defined such that the back of the Pisa-IIT Softhand approaches the object. Forces pushing the fingers to the front move the fingers independently of each other as the tendon connecting all of them is not stretched. So they are uncoupled, making the hand behave as a single spring.

For the adaptive grasping action the joint states of the fingers are coupled because the tendon connecting all of them is pulled, which leads to an adaptive grasp, which could be helpful filling the space in the close to a irregular surface, like in a grasp on the rim close to the handle of the mug.

The poking action is not adaptive but has the advantage of exploring holes, what can be helpful if containers are used as objects.

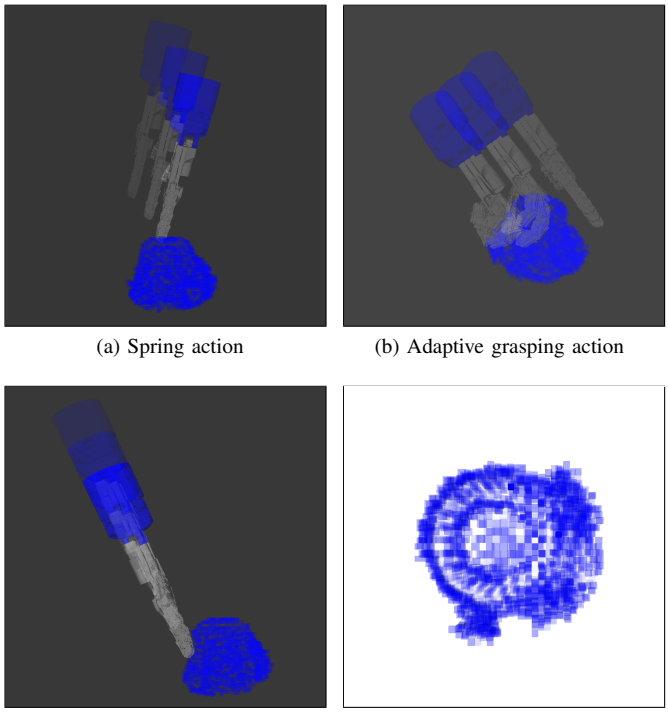

(a) Spring action (b) Adaptive grasping action

(c) Poking action (d) Occupancy grid posterior

Fig. 2: (a-c) Three different action primitives. (d) Occupancy grid posterior of the mug belief. The percentage of transparency of the cells is proportional to the occupancy probability. Before building the posterior a uniform occupancy prior was assumed.

V. CONCLUSION

So far we implemented the occupancy aware pose distribution sampling, computation of the occupancy grid posterior and the definition of the action primitives. In the future we want to finish implementation and show results in both simulation and on our robot. We want to compare the effectiveness of the different action primitives in refining the pose belief in scenarios with objects having different masses and sizes and different levels of occlusion. It might also be worth to investigate scenes containing a set of different objects.

REFERENCES

[1] P. K. Allen and R. Bajcsy. *Object recognition using vision and touch*. PhD dissertation: University of Pennsylvania, 1985.

[2] T. Arbel and F. P. Ferrie. Entropy-based gaze planning. *Image and Vision Computing*, 19(11):779–786, sep 2001.

[3] J. Bimbo, P. Kormushev, K. Althoefer, and H. Liu. Global estimation of an object's pose using tactile sensing. *Advanced Robotics*, 29(5):363–374, 2015.

[4] M. G. Catalano, G. Grioli, E. Farnioli, A. Serio, C. Piazza, and A. Bicchi. Adaptive synergies for the design and control of the Pisa/IIT SoftHand. *The International Journal of Robotics Research*, 33(5):768–782, Apr. 2014.

[5] A. Davison. Active search for real-time vision. In *Tenth IEEE International Conference on Computer Vision (ICCV'05) Volume 1*, volume 1, pages 66–73 Vol. 1. IEEE, 2005.

[6] R. Detry, D. Kraft, O. Kroemer, L. Bodenhagen, J. Peters, N. Krüger, and J. Piater. Learning grasp affordance densities. *Paladyn. Journal of Behavioral Robotics*, 2011. accepted.

[7] R. Detry and J. Piater. Continuous surface-point distributions for 3D object pose estimation and recognition. In *Asian Conference on Computer Vision*, pages 572–585, 2010.

[8] W. E. L. Grimson and T. Lozano-Perez. Model-Based Recognition and Localization from Sparse Range or Tactile Data. *The International Journal of Robotics Research*, 3(3):3–35, sep 1984.

[9] P. Hebert, T. Howard, N. Hudson, J. Ma, and J. W. Burdick. The next best touch for model-based localization. In *2013 IEEE International Conference on Robotics and Automation*, pages 99–106. IEEE, may 2013.

[10] K. Hsiao, L. Kaelbling, and T. Lozano-Perez. Task-driven tactile exploration. In *Proceedings of Robotics: Science and Systems*, Zaragoza, Spain, June 2010.

[11] M. Krainin, B. Curless, and D. Fox. Autonomous generation of complete 3D object models using next best view manipulation planning. In *2011 IEEE International Conference on Robotics and Automation*, pages 5031–5037. IEEE, may 2011.

[12] J. Ma and J. Burdick. Sensor planning for object pose estimation and identification. In *2009 IEEE International Workshop on Robotic and Sensors Environments*, pages 69–74. IEEE, nov 2009.

[13] A. Petrovskaya and O. Khatib. Global Localization of Objects via Touch. *IEEE Transactions on Robotics*, 27(3):569–585, jun 2011.

[14] C. Strub, F. Worgotter, H. Ritter, and Y. Sandamirskaya. Correcting pose estimates during tactile exploration of object shape: a neuro-robotic study. In *4th International Conference on Development and Learning and on Epigenetic Robotics*, pages 26–33. IEEE, oct 2014.

[15] N. Tosi, O. David, and H. Bruyninckx. Action selection for touch-based localisation trading off information gain and execution time. In *2014 IEEE International Conference on Robotics and Automation (ICRA)*, pages 2270–2275. IEEE, may 2014.

[16] L. L. S. Wong, L. P. Kaelbling, and T. Lozano-Perez. Not seeing is also believing: Combining object and metric spatial information. In *Robotics and Automation (ICRA), 2014 IEEE International Conference on*, pages 1253–1260. IEEE, May 2014.

[17] C. Zito, M. S. Kopicki, R. Stolkin, C. Borst, F. Schmidt, M. A. Roa, and J. L. Wyatt. Sequential trajectory re-planning with tactile information gain for dexterous grasping under object-pose uncertainty. In *2013 IEEE/RSJ International Conference on Intelligent Robots and Systems*, pages 4013–4020. IEEE, nov 2013.